Environmental Research 223 (2023) 115488

Contents lists available at ScienceDirect

Environmental Research

journal homepage: www.elsevier.com/locate/envres

Response of OC, TN, and TP deposition mediated by aquatic photosynthetic community structures in shallow karst surface waters under different land uses

Qian Bao [a,b,c], Zaihua Liu [b,c,*], Min Zhao [b,c], Hailong Sun [b], Yundi Hu [d], Dong Li [b], Cheng Zeng [b], Yu Wei [b,e], Yi Zhang [b,c], Haibo He [b,c]

[a] Key Laboratory of Land Resources Evaluation and Monitoring in Southwest, Ministry of Education,Sichuan Normal University,Chengdu, 610066, China
[b] State Key Laboratory of Environmental Geochemistry, Institute of Geochemistry, CAS, Guiyang, 550081, China
[c] Puding Karst Ecosystem Research Station, Chinese Ecosystem Research Network, CAS, Puding, 562100, Guizhou, China
[d] School of Geography and Environmental Science, Guizhou Normal University, Guiyang, 550025, China
[e] School of Earth Sciences and Engineering, Nanjing University, Nanjing, 210093, China

ARTICLE INFO

Handling Editor: Robert Letcher

Keywords:
C–N–P deposition
Aquatic photosynthetic
Community structures
Shallow karst surface waters
Land uses

ABSTRACT

Land use change alters the hydrochemical features, nutrient outputs, and community structure of aquatic photosynthetic organisms in watersheds and has an important impact on C, N, and P biogeochemical processes. In shallow water environments, sediments are the most important burial sites for C, N, and P; however, the factors underlying the control of their deposition by land use changes remain unclear. In this study, the relationship among hydrochemical features, aquatic photosynthetic organism community structure, and C, N, and P deposition in surface waters associated with different land uses was studied at the Shawan Karst Water-Carbon Cycle Test Site, Puding, SW China, by combining field monitoring and laboratory experiments performed over a complete hydrological year from September 2018 to August 2019. The results indicate that (1) OC and TN deposition showed small differences among ponds associated with five land uses, while TP was significantly higher in ponds associated with shrubland and grassland than in ponds of cultivated land, bare soil, and bare rock. (2) Cultivated land increased OC and TN deposition by increasing N and P output and planktonic algae biomass in surface waters, while grassland and shrubland ponds mainly by increasing DIC output and macrophyte biomass. (3) Compared with cultivated land, grassland and shrubland significantly enhanced TP deposition by promoting the deposition of calcium-bound P and biogenic P from macrophytes and their epiphytic algae in surface waters. In conclusion, the shift of cultivated land and bare soil to grassland and shrubland may be conducive to the formation of benign aquatic ecosystems and stabilization of C, N, and P sinks in karst shallow surface waters.

1. Introduction

Land use and land cover change represents one of the main drivers underlying changes in the biogeochemical cycles of biogenic elements and the community structure of aquatic ecosystems (Howarth et al., 2011; Hayes et al., 2015). Previous studies have shown that an increase in the proportion of cultivated and building land promotes the output of nitrogen (N) and phosphorus (P) in a watershed (Luo et al., 2020). Natural vegetation restoration or artificial forest and grass cultivation can reduce the output of N and P to a watershed, thereby increasing the dissolved inorganic carbon (DIC) concentration and water transparency (Cruz et al., 2015; Bao et al., 2020). Moreover, the physicochemical parameters of surface water, such as electrical conductivity (EC), calcite saturation index (SIc), and Ca^{2+}, also show differences under different land use patterns (Zhao et al., 2010; Chen et al., 2017; Wang et al., 2020b). As the N and P outputs to surface water in a watershed increase, the primary productivity of planktonic algae in rivers, reservoirs, lakes, and oceans significantly increases, which triggers eutrophication (Howarth and Marino, 2006; Schindler et al., 2016). In contrast, higher water transparency and DIC concentrations can promote macrophyte growth, thereby inhibiting the growth of planktonic algae to some extent (Jones et al., 2002; Dülger et al., 2017). Overall, changes in water

---

* Corresponding author. State Key Laboratory of Environmental Geochemistry, Institute of Geochemistry, CAS, Guiyang, 550081, China.
E-mail addresses: 1505523145@qq.com (Q. Bao), liuzaihua@vip.gyig.ac.cn (Z. Liu).

https://doi.org/10.1016/j.envres.2023.115488
Received 7 December 2022; Received in revised form 7 February 2023; Accepted 10 February 2023
Available online 11 February 2023

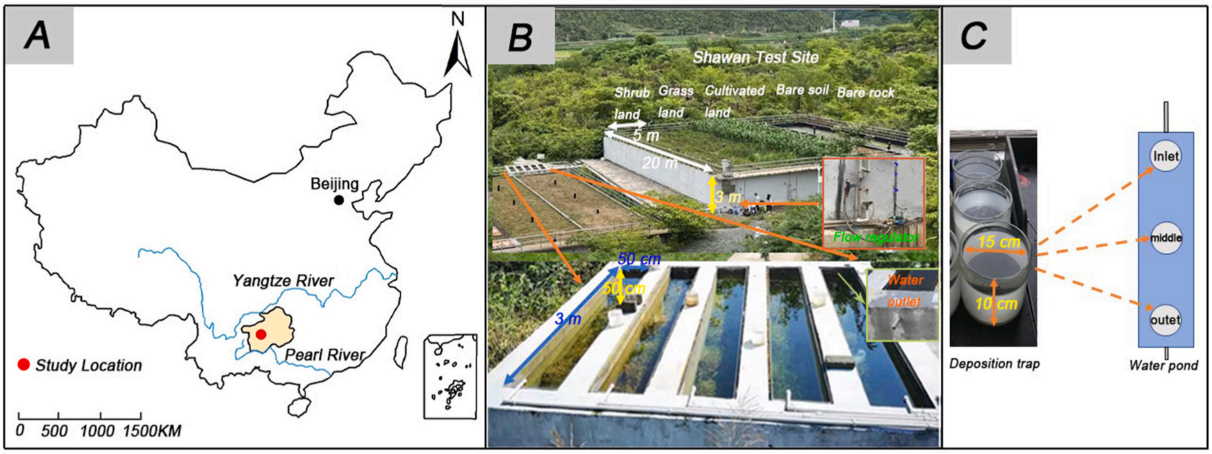

Fig. 1. (A) Location of the Shawan Karst Water-carbon Cycle Test Site; (B) five tank watersheds with their different land uses: bare rock, bare soil, cultivated land (corn), grass land (alfalfa), and shrub land (Roxburgh roses); and (C) deposition traps and their deployment location (inlet, middle, and outlet).

physicochemical parameters and nutrients mediated by different land use patterns may affect the biomass of phytoplankton and macrophytes and regulate the succession of biological structures (Hayes et al., 2015). Additionally, researchers have found that the succession of the aquatic photosynthetic community structure has an important influence on the burial of organic carbon (OC), N, and P in surface water systems (Brothers et al., 2013; Némery et al., 2016; Klamt et al., 2019).

Lakes, reservoirs, and ponds are important sinks for C, N, and P in inland waters worldwide, thus reducing nutrient transport from inland to the ocean (Seitzinger et al., 2010; Némery et al., 2016; Rogers et al., 2022). Reservoirs and lake water are relatively static, which promotes the growth of aquatic organisms and results in a higher proportion of autochthonous OC, N, and P burial in the sediment (Zhang et al., 2017; Huang et al., 2018; He et al., 2020). The large amounts of N and P entering surface waters during agricultural intensification have led to widespread eutrophication in European lowland lakes, and studies on lake sediments have found that eutrophication in these lakes has led to a four-to five-fold increases in OC stocks (Smith , 2003; Anderson et al., 2014). Previous studies on total nitrogen (TN) in sediments shows that TN in different age layers generally shows a trend consistent with that of OC; thus, these elements presents a certain coupling relationship in the production and sedimentation processes (Némery et al., 2016; Huang et al., 2018; Zhao et al., 2021). However, P deposition is influenced by aquatic organisms and also co-precipitates with Ca^{2+}, Al^{3+}, and Fe (III)-humic complexes in water; thus, it generally shows different trends from OC and TN (O'Connell et al., 2020; Wen et al., 2022). Klamt et al. (2019) found that the shift from macrophyte to phytoplankton dominance led to a 1.8-fold increase in the sediment accumulation rate of total phosphorus (TP), especially biogenic P (NaOH-extracted NRP) and Al-bound P (NaOH-extracted SRP). In Taihu Lake, where macrophytes are dominant relative to phytoplankton, calcium-bound P (Ca–P) and residual P are the dominant elements in the sediment (Zhang et al., 2017), which indicates that the biological structure of the waterbody has an important influence on the form and amount of P deposition (Brenner et al., 2006; Urbaniak, 2010; Yuan et al., 2020). Furthermore, studies of lakes and reservoirs in karst areas have indicated that the sediments contain high levels of Ca–P owing to the high content of Ca^{2+} and DIC in the surface water (Sun et al., 2022). Nevertheless, the influence of structural changes in aquatic photosynthetic organisms on C, N, and P deposition in karst shallow-water environments with high Ca^{2+} and DIC concentrations needs to be further elucidated (Bao et al., 2022).

Karst landscapes are widely distributed and cover approximately 15% of the global land surface area, and approximately 20% of the world's population live within karst regions (Ford and Williams, 2013; Chen et al., 2020). The karst region of Southwest China (KRSC) is the largest continuous karst area in the world, and due to long-term high-intensity human reclamation and destruction, a series of ecological and environmental problems, such as vegetation destruction, soil erosion, and productivity decreases, have become prominent (Yan et al., 2018; Chen et al., 2020; Li et al., 2021). In recent years, under the initiative of local governments, large-scale afforestation and farmland return to forest and grassland projects have been widely carried out (Yue et al., 2020). Previous studies have extensively studied a series of soil ecological effects, such as soil erosion, nutrient loss, and soil carbon sequestration after revegetation, and found that fragile ecosystems are protected and restored by such projects (Wang et al., 2004; Hu et al., 2016; Tong et al., 2018). Moreover, researchers found that planting grassland and shrubland promoted C fixation and increased the biomass of submerged plants in surface waters (Chen et al., 2017; Bao et al., 2022). However, the effects of vegetation restoration on C, N, and P deposition in aquatic ecosystems have not been extensively studied and require further in-depth research (Liu et al., 2021).

Here, this study systematically investigated the hydrochemistry, nutrient, aquatic photosynthetic community, and C, N, and P deposition characteristics in the surface waters of five simulated spring-pond systems with different land use patterns (bare rock, bare soil, cultivated land, grassland, and shrubland) to answer the following three questions: (1) Does C, N, and P deposition differ under different land use patterns? (2) How is the structure of aquatic photosynthetic organisms correlated with C, N, and P deposition? (3) How does land use regulate C, N, and P deposition in shallow karst surface waters? And hypothesized that vegetation restoration is conducive to C, N, and P burial and stabilization in karst aquatic ecosystems, which has significant implications for eutrophication control and carbon neutralization, thus representing a win-win situation.

2. Materials and methods

2.1. *Description of the study site*

The Shawan Karst water-carbon cycle test site (26°14′–26°15′N, 105°42′–105°43′E) is located at the National Observation Station of the Karst Ecosystem in Puding County, Guizhou Province, China (Fig. 1A). It has a typical humid subtropical monsoonal climate with a mean annual air temperature of 15.2 °C, mean annual precipitation of 1341 mm (80% of which occurs from May to August), and mean annual relative humidity of 78% (Zhao et al., 2010). Five concrete tanks were built to simulate natural watersheds with identical hydrogeological conditions (bedrock and watershed boundaries) but different land covers: bare rock, bare soil, cultivated, grass, and shrub lands (Fig. 1B). Each

Table 1
Aquatic photosynthetic community characteristics in pond water under five land uses.

Physiochemical and biological parameters	Bare rock	Bare soil	Cultivated land	Grassland	Shrubland					
	Dormant period	Growth period	Dormant period	Growth period	Dormant period	Growth period	Dormant period	Growth period	Dormant period	Growth period
C/N algae	9.41	9.62	9.14	9.21	10.14	9.97-	10.88	12.75	10.35	11.87
C/N plant	14.34	11.77	14.10	13.12	13.93	12.18-	17.30	16.28	25.68	23.28
$\delta^{13}C_{algae}$ (‰, VPDB)	−23.62	−16.78	−24.73	−16.58	−28.86	−27.82	−36.39	−34.11	−31.89	−32.13
$\delta^{13}C_{plant}$ (‰, VPDB)	−12.77	−14.75	−16.38	−18.02	−19.05	−18.47	−24.93	−22.16	−21.94	−19.52
accumulation of monthly Chl-a (ug L-1)	3.43	6.22	4.39	9.15	7.28	8.58	4.35	5.18	3.82	5.45
accumulation of monthly DW (mg cm-1)	4.70	7.81	6.84	9.27	9.94	12.06	13.42	18.23	8.78	17.43

DW is the dry weight of submerged plants.

concrete tank was 20 m long, 5 m wide, and 3 m deep, and they were coated with epoxy resin to avoid the influence of possible concrete erosion on the tank hydrochemistry and then filled with dolomitic limestone gravel (2.5 m) (Chen et al., 2017). The first of these tanks was used to simulate bare rocks; the second was filled with 0.5 m local soil on dolomitic limestone gravel to simulate bare soil, and the remaining three were filled with the above rocks, topped with 0.5 m local soil, and then planted with corn, alfalfa, and roses to simulate cultivated, grass, and shrubs, respectively. Details on the chemical composition of the rock and soil materials can be found in Zeng et al. (2017). Corn was planted annually and buried in the soil after harvest, and the alfalfa and Roxburgh roses were planted in January 2014. The corn plants grew from April to August and were treated with compound fertilizer ($N + P + K \geq 45\%$, 0.01 kg m^{-2}) during the growth. Furthermore, water was drained with a polyvinyl chloride pipe at the end of each tank to simulate a natural karst spring to feed an artificial pond, which was 3 m long, 0.5 m wide, and 0.5 m deep (Fig. 1B). To ensure that the spring water maintained a perennial flow year-round, each drainage outlet was equipped with a flow regulator. Planktonic algae and submerged plants (mainly Chara spp.) were collected from a nearby river and transplanted them evenly into each pond to simulate a shallow natural lake or reservoir in August 2018. After the system was stabilized, deposition traps made of Plexiglas with a bottom diameter of 15 cm and a height of 10 cm to collect the deposition be placed at the inlet, middle, and outlet in each pond (Fig. 1C). More detailed information about the simulated ecosystem can be found in Bao et al. (2022).

2.2. *Field monitoring*

The study began in September 2018 and ended in August 2019. A sunny day was chosen for water monitoring and sample collection at the end of each month except for July 2019, when the instrument was damaged and needed repair. The hydrochemical parameters of temperature (T), pH, electrical conductivity (EC, 25 °C), and dissolved oxygen (DO) were monitored using a multiparameter water quality probe (Wissenschaftlich-Technische Werkstaetten Technology Multiline 350i, Germany) (Bao et al., 2020). The instrument was calibrated for pH, DO, and EC before each test. Moreover, DIC was titrated with an Aquamerck alkalinity test kit (Merck, Germany), and the estimated accuracy was 0.1 mmol L^{-1} (Zeng et al., 2017).

2.3. *Sample collection and laboratory measurements*

The water samples collected monthly from the spring and pond waters were measured for TN, TP, NO_3^-, PO_4^{3-}, chlorophyll-a (Chl-a), Ca^{2+}, total OC (TOC), and $\delta^{13}C_{DIC}$. Planktonic algal samples were collected during each season for qualitative and quantitative analyses. In addition, because of the large amount of planktonic algal biomass required to determine the molar C/N ratios and OC isotopes, the study combined planktonic algal samples from each sample pond collected over four seasons for measurement. Furthermore, the biomass, C/N, and OC isotopes of submerged plants be determined during two periods from September 2018 to March 2019 and from April to August 2019. Detailed collection and measurement methods can be found in Bao et al. (2022).

Deposition samples were collected from the traps at the end of March and August 2019, transported to the laboratory to aspirate excess water with a syringe, and then freeze-dried. After the dry weight was measured, parts of the samples were obtained, ground evenly, and then filtered through a 200-mesh sieve. The sieved samples were then acidified with 2 mol/L hydrochloric acid in a 50 ml centrifuge tube for 12 h, centrifuged, and washed with ultrapure water, and the cleaned samples were freeze-dried. After drying, the C/N and OC isotopes of the samples were determined using an Elementar Vario Macro cube (Elementar, Germany) and MAT-252/253 mass spectrometer (Thermo Fisher Scientific Inc., USA) (He et al., 2020). Partially sieved samples were collected, and the TP concentration in the deposition was determined by the SMT method (Ruban et al., 2001). Based on the deposition of OC, TN, and TP and the bottom area of the trap, the amount of deposition per unit area were calculated. Finally, the Ca–P content of the deposition was determined by sequential extraction fractionation (Hupfer et al., 1995).

2.4. *Data analyses*

Origin Pro2018 was used for correlation analyses and figure drawing. The dissolved CO_2 (CO_2(aq)) concentration in the water was calculated using PHREEQC based on the pH, T, and HCO_3^- concentrations, whereas SIc was calculated using PHREEQC based on the pH, T, K^+, Na^+, Ca^{2+}, Mg^{2+}, HCO_3^-, Cl^-, SO_4^{2-}, and NO_3^- concentrations (Sun et al., 2022). Moreover, we used IBM SPSS Statistics 24 to perform one-way ANOVAs with the LSD test after passing the normal test and homogeneity of variance tests ($P > 0.05$).

3. Results

3.1. *Physiochemical and aquatic photosynthetic parameter characteristics in water*

Considering the growth cycle of aquatic photosynthetic organisms, this study divided the experimental period into dormant period (from September 2018 to March 2019) and growth period (April to August 2019). The physiochemical (T, pH, DO, EC, Ca^{2+}, SIc, pCO_2, DIC, N, and P) characteristics in the spring and pond waters under different land uses are shown in Tables S1 and S2. The water under shrubland and grassland showed higher HCO_3^-, CO_2(aq), and Ca^{2+} and lower TN and TP concentrations. Cultivated land showed lower HCO_3^-, CO_2(aq), and Ca^{2+} and higher TN and TP concentrations. Bare rock and bare soil showed low HCO_3^-, CO_2(aq), and Ca^{2+} and medium TN and TP concentrations. The aquatic photosynthetic parameter (biomass, C/N, and $\delta^{13}C_{oc}$) are shown in Table 1. The highest accumulation of monthly Chl-a

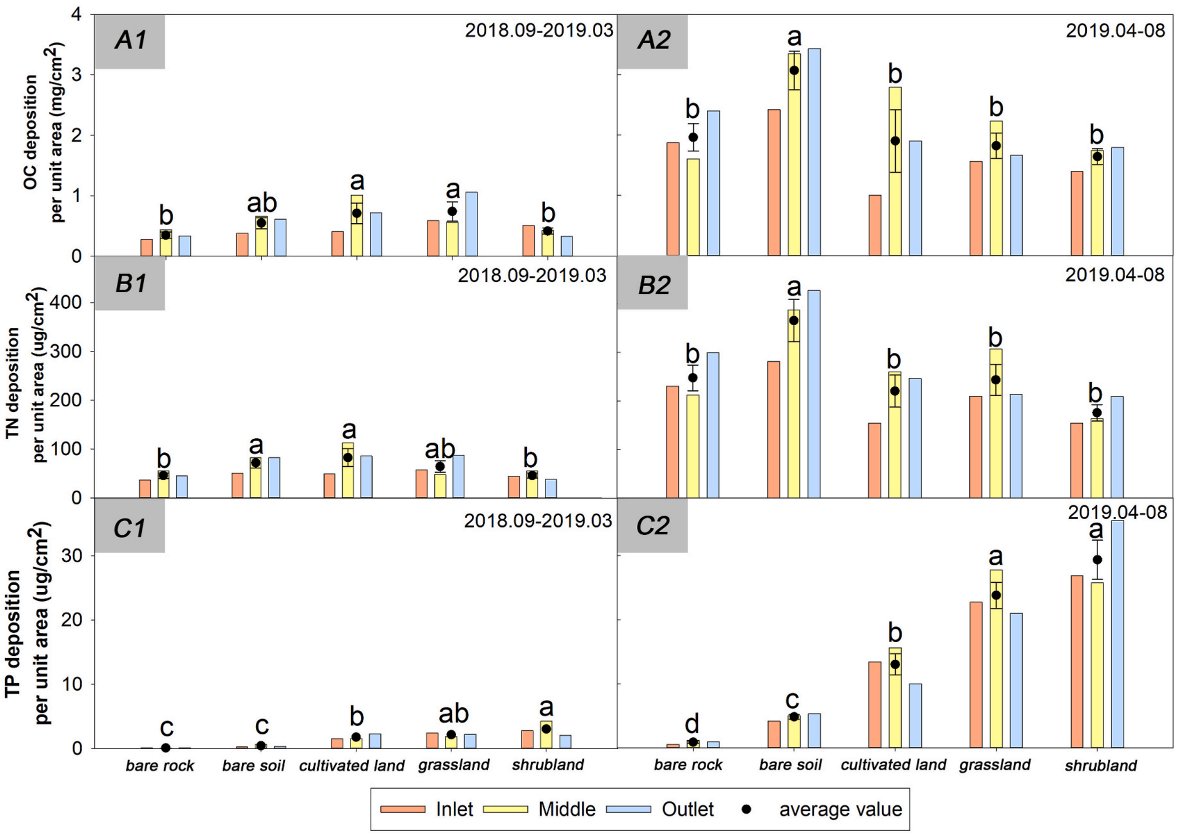

Fig. 2. (A1, A2) OC deposition per unit area from September 2018 to March 2019 and April 2019 to August 2019, respectively; (B1, B2) TN deposition per unit area from September 2018 to March 2019 and April 2019 to August 2019, respectively; (C1, C2) TP deposition per unit area from September 2018 to March 2019 and April 2019 to August 2019, respectively. The different lowercase letters above the bars (for a, b, c, d) represent significant differences among the five ponds (one-way ANOVA with LSD test, $P < 0.05$).

concentration occurred in the cultivated land pond during growth period, with the value of 9.15 μg/L, while the grass and shrub lands showed lowest values with 5.18 and 5.45 μg/L, respectively. The highest accumulation of monthly biomass of submerged plants (18.23 mg/cm^2) occurred in the grassland pond during growth period, while lower values were observed for bare rock and bare soil (7.81 and 9.27 mg/cm^2), respectively. The C/N ratio of planktonic algae showed small differences under different land uses, with values ranging from 9.14 to 12.75. However, the C/N of submerged plants showed some differences, higher in grassland and shrubland, lower in bare rock and soil. Moreover, it found that the OC isotope ($\delta^{13}C_{OC}$) values were slightly positive in cultivated land, bare soil, and bare rock ponds but more negative in shrubland and grassland ponds.

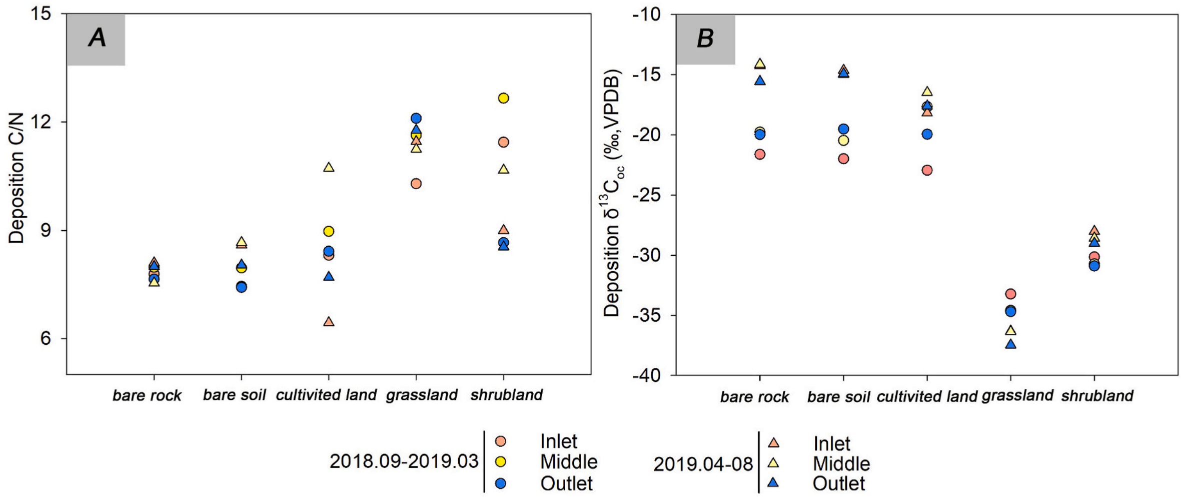

Fig. 3. (A) C/N (molar ratio) and (B) organic carbon isotopes of deposition under different land uses from September 2018 to March 2019 and April 2019 to August 2019.

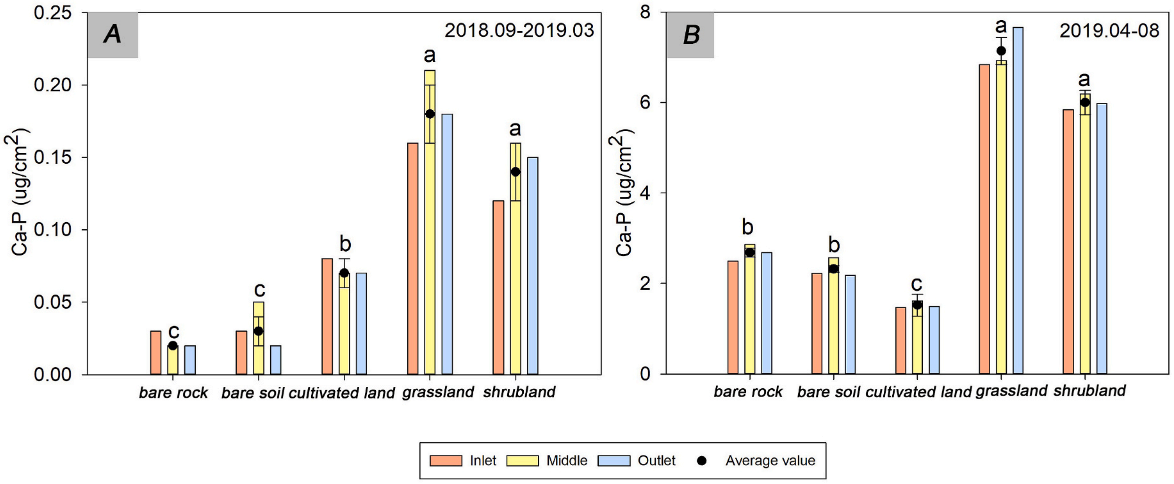

Fig. 4. Calcium-bound phosphorus (Ca–P) deposition per unit area under different land uses from September 2018 to March 2019 (A) and April 2019 to August 2019 (B). The different lowercase letters above the bars (for a, b, c) represent significant differences among the five ponds (one-way ANOVA with LSD test, $P < 0.05$).

3.2. *Total deposition in surface water under different land uses*

The deposition samples and deposition amount per unit area are shown in Fig. S1. Fig. S1A shows that there was a large amount of submerged plant debris in the traps under grass and shrubs, while planktonic algae debris was mainly observed under cultivated land, bare soil, and bare rock. Moreover, there showed small differences in the deposition per unit area of surface water under the five land uses during both the dormant and growth periods (Figs. S1B and S1C).

3.3. *Characteristics of C, N, and P deposition*

By measuring the OC, TN, and TP concentrations of the deposition samples, the OC, TN, and TP deposition per unit area were calculated in the pond waters under the five land uses, as shown in Fig. 2. During the dormant period, OC deposition in the ponds under cultivated land and grassland was significantly higher than that under shrubland and bare rock (Fig. 2 A1). TN deposition in ponds under cultivated land and bare soil was significantly higher than that under shrubland and bare rock (Fig. 2 B1). During the growth period, it found that OC and TN deposition exhibited similar characteristics in the five ponds (Fig. 2 A2, B2). The OC and TN deposition in the bare soil pond was significantly higher than that of the other four land uses, while that of the other four land uses did not show significant differences.

The deposition of TP was significantly different from that of OC or TN and shown in Fig. 2C. In the dormant period, TP deposition in the shrubland pond was significantly higher than that in the cultivated land, bare soil, and bare rock ponds, whereas that in the grassland pond was not significantly different from that of the shrubland and cultivated land ponds (Fig. 2 C1). Moreover, TP deposition in the ponds under bare soil and bare rock was significantly lower than that under the other three land uses. During the growth period, TP deposition in the shrubland and grassland ponds were significantly higher than that in the cultivated land pond, which was significantly higher than that of bare soil and bare rock ponds (Fig. 2 C2).

3.4. *C/N, organic carbon isotope, and Ca–P content in deposition*

To examine the sources of OC and N in the deposits, the C/N and OC isotopes ($\delta^{13}C_{oc}$) of the deposits were measured in the five land use ponds, and the results are shown in Fig. 3. In the dormant period, the average values of C/N deposition exhibited the following trend: shrubland > grassland > cultivated land > bare rock > bare soil. During the growth period, the average values of C/N deposition exhibited different trends: grassland > shrubland > bare soil > cultivated land > bare rock. In general, the values of C/N deposition in the ponds under grassland and shrubland were higher than those under the other three land uses (Fig. 3A). As shown in Fig. 3B, the $\delta^{13}C_{oc}$ values of the deposits under the five land uses showed the same trend during the two sampling periods. Grassland and shrubland were more negative than cultivated, bare soil, and bare rock.

In Fig. 2, the deposition of TP showed a different trend from that of OC and TN. Furthermore, the co-precipitation of calcium carbonate and phosphorus in karst surface waters makes an important contribution to the deposition of TP, the Ca–P content in the deposits were measured and shown in Fig. 4. In the dormant period, the Ca–P content in the grassland and shrubland ponds were significantly higher than that of and cultivated land pond, and the latter was significantly higher than those of the bare soil and bare rock ponds (Fig. 4A). During the growth period, the Ca–P deposition trends under different land uses differed from that of the dormant period. The Ca–P content in grassland and shrub ponds were significantly higher than that of the bare soil, bare rock, and cultivated land ponds (Fig. 4B). Interestingly, the deposition of both TP and Ca–P were high in grassland and shrub ponds with extremely low phosphorus concentrations in the water (Table 1, Fig. 2C).

4. Discussion

4.1. *Influence of phytoplankton and submerged plants on OC and TN deposition in pond*

Generally, OC and TN in sediment are mainly derived from terrestrial plants, soil, plankton, and macrophytes (Huang et al., 2020). In inland waters, OC and TN derived from aquatic photosynthetic organisms represent an important part of the sediments, especially in karst lakes, where autochthonous OC has been shown to account for more than 60% (Huang et al., 2018; He et al., 2020). Moreover, researchers found that OC and TN burial is influenced by the succession between macrophyte and phytoplankton communities (Brothers et al., 2013; Wang et al., 2016). Our results showed that the relationship between the cumulative planktonic algal biomass (accumulation of monthly Chl-a values) and deposited OC or TN content per unit area ($r^2 = 0.61$, $P < 0.01$; $r^2 = 0.57$, $P < 0.01$) was better than that in submerged plants ($P > 0.05$) (Fig. S2). Although planktonic algae tend to be decomposed faster than submerged plants, the high productivity of algae can also lead to greater organic matter deposition (Enríquez et al., 1993; Hilton et al., 2006). Moreover, the reason for the high productivity of planktonic algae is that

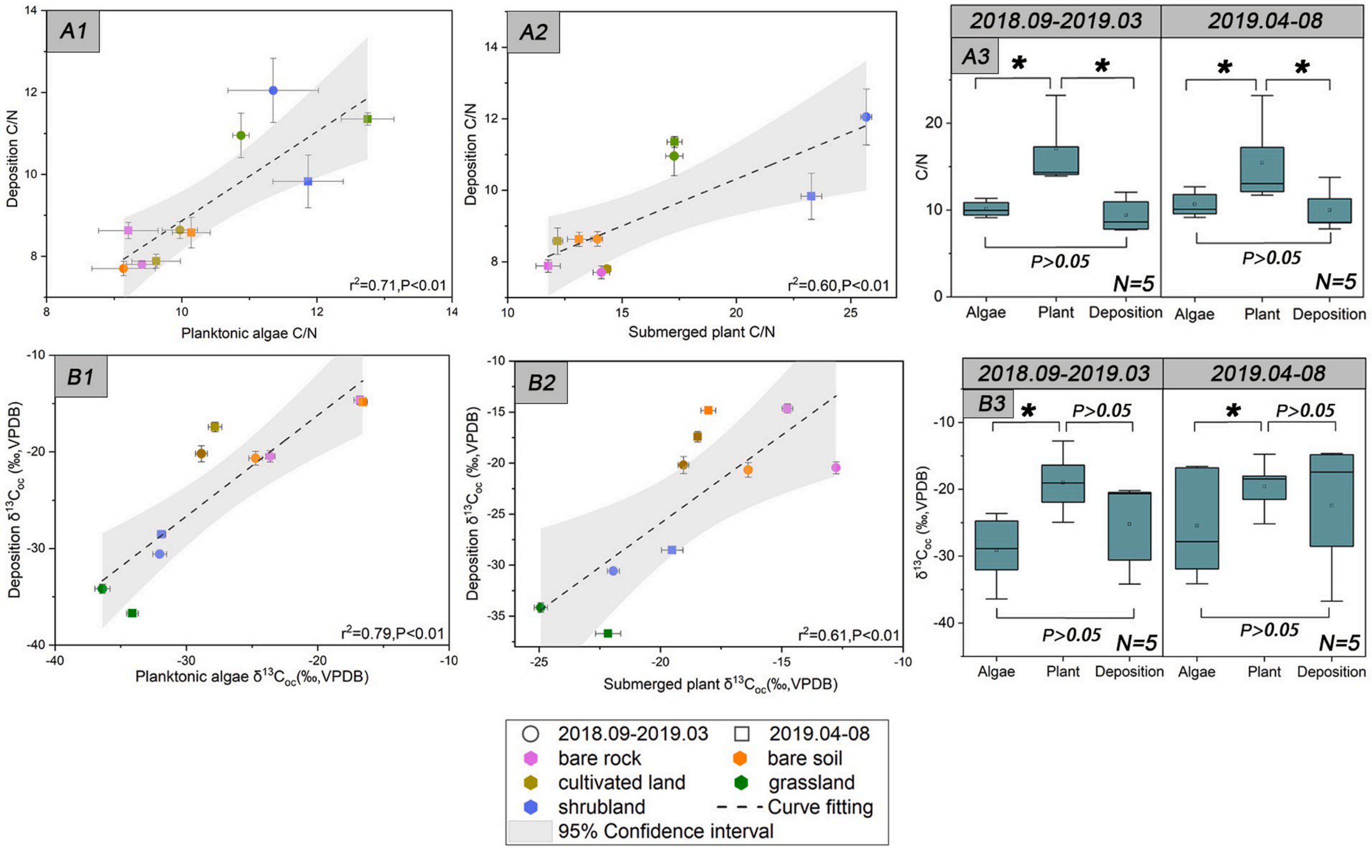

Fig. 5. Relationships between the C/N and organic carbon isotopes values ($\delta^{13}C_{oc}$) of planktonic algae (A1, B1) and submerged plants (A2, B2) in the pond water and the C/N and organic carbon isotopes ($\delta^{13}C_{oc}$) of deposition, respectively. A3 and B3 present the ANOVA analysis results for C/N and $\delta^{13}C_{oc}$ in planktonic algae, submerged plants, and deposition, respectively. * Significant difference; $P > 0.05$ indicates no significant differences.

these organisms are more competitive than plants in terms of light and nutrients (O'Hare et al., 2018). Thus, our preliminary results support Downing et al. (2008)'s view that OC and TN in deposition are mainly derived from planktonic algae. However, studies have found that different degradation rates of planktonic algae and submerged plants could lead to differences in the OC and TN contents in sediments (Asaeda et al., 2007; Thomas et al., 2011). Therefore, the relationship between cumulative biomass and OC or TN deposition in this study may not truly reflect the contribution of planktonic algae and submerged plants to OC and TN deposition; thus, these relationships require further study.

C/N and carbon isotopes are commonly used tools to study the sources of OC and N in sediments (Meyers, 1994; He et al., 2020). To further study the effects of planktonic algae and submerged plants on OC and TN deposition, this study analyzed the OC isotope and C/N of planktonic algae and submerged plants, as shown in Fig. 5. The C/N ratio of planktonic algae ($r^2 = 0.71$, $P < 0.01$) and submerged plants ($r^2 = 0.60$, $P < 0.01$) had a significant linear positive correlation with the C/N ratio of deposition (Fig. 5 A1, A2). However, the C/N ratio of submerged plants was generally higher than that of planktonic algae and deposition. Moreover, the ANOVA results showed that the C/N ratio of submerged plants was significantly different from C/N deposition ($P < 0.05$), while the C/N ratio of planktonic algae and deposition were similar and did not show a significant difference ($P > 0.05$) (Fig. 5 A3). Anderson et al. (2014) found that algal blooms in recent European lakes led to a three-to four-fold increase in the OC in sediments. This study also indicates that the OC in the deposition may be mainly from planktonic algae. In addition, it found that the $\delta^{13}C_{oc}$ values of planktonic algae ($r^2 = 0.79$, $P < 0.01$) and submerged plants ($r^2 = 0.61$, $P < 0.01$) also showed a significant linear positive correlation with deposition (Fig. 5 B1, B2). However, an interesting phenomenon was observed: although planktonic algae and submerged plants showed significant differences in OC isotope values, neither of them showed a significant difference from the deposition values (Fig. 5 B3). Hunter (1976) reported that the values of C/N could decrease from 19.3 to 8.3 during the decomposition of Chara spp. Moreover, ponds with lower planktonic algal biomass and higher submerged plant biomass did not show significant differences in OC deposition from ponds with higher planktonic algal biomass and lower submerged plant biomass (Table 1, Fig. 2 A, B). Therefore, we inferred that OC in the deposits was contributed by both planktonic algae and submerged plants and the relative biomass of planktonic algae and submerged plants determines the main source of OC. Finally, we believe that the major source of TN deposition per unit area in this study was the same as that of OC because TN and OC generally have similar trends in sediments (Huang et al., 2018; Liu et al., 2021, Fig. 2 A, B). Although Brothers et al. (2013) found that the shift from macrophyte to phytoplankton dominance enhances carbon burial in a shallow eutrophic lake, our previous study (Bao et al., 2022) and this study suggested that higher DIC concentrations in karst shallow surface waters can enhance OC and TN deposition by increasing submerged plant biomass, and such dynamics should be considered when studying autochthonous OC and TN sinks in sediments.

4.2. *Influence of phytoplankton and submerged plants on P deposition in ponds*

As a major limiting nutrient for primary productivity in inland water, P can promote the proliferation of planktonic algal biomass and lead to the formation of algal blooms (Carvalho et al., 2013; Schindler et al., 2016). Aquatic photosynthetic organisms also contribute to P sinks in reservoirs and lakes by absorbing phosphorus in water and becoming

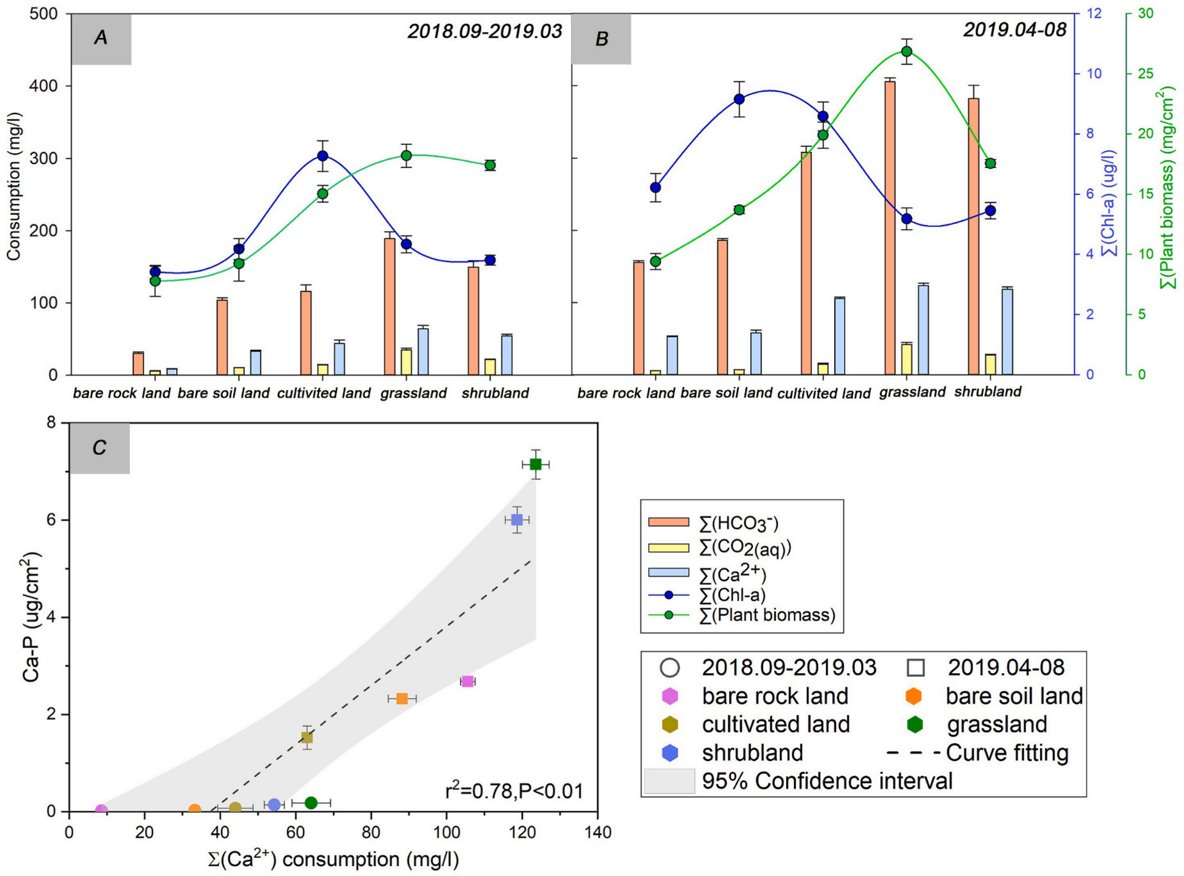

Fig. 6. Cumulative consumption of HCO_3^-, $CO_{2(aq)}$, and Ca^{2+}, and cumulative biomass of planktonic algae and submerged plants in the pond water from September 2018 to March 2019 (A) and April 2019 to August 2019 (B); (C) relationship between the cumulative consumption of Ca^{2+} and Ca–P deposition per unit area.

incorporated in sediments after death (Carpenter et al., 1992; O'Connell et al., 2020). Moreover, Klamt et al. (2019) found that the shift from macrophyte to phytoplankton dominance could change the P form and burial. We studied this shift, and the results are shown in Fig. S3. We found that the cumulative submerged plant biomass showed a significant linear positive correlation with TP deposition per unit area ($r^2 = 0.46$, $P = 0.03$), whereas planktonic algae did not show a significant correlation with this factor ($P > 0.05$). This finding indicates that submerged plants appear to contribute more to TP deposition. This conclusion was supported by the fact that TP deposition was significantly higher in the ponds with low algae and high submerged plant biomass (Table 1, Fig. 2C). However, previous studies have found that planktonic algal blooms significantly increase phosphorus burial in sediments (Yuan et al., 2020; Rogers et al., 2022), which may be explained by the differences in the size of phytoplankton and submerged plant biomass and their influence on the production of different forms of phosphorus (Brezonik and Engstrom, 1998; Klamt et al., 2019). Phosphorus contributed by algal debris is mainly in the form of biological P (NaOH–P), which easily returns to the water column in the form of active P during microbial degradation (Zhang et al., 2017). Due to the slow degradation rate of debris, submerged plants can promote the binding of some P released from iron-bound P and biological P to calcium complexes by producing large amounts of O_2, absorbing HCO_3^-, and providing adsorption sites, thereby producing refractory P fractions (including HCl–P and residual P) (Urbaniak, 2010; Xu et al., 2013; Klamt et al., 2019). Previous studies indicated that large amounts of calcite precipitation occur during biological carbon pumping (BCP) in karst surface waters (Liu et al., 2018), which promoted the co-precipitation of large amounts of active P with calcite (Murphy et al., 1983). Sun et al. (2022) found that Ca-bound P (Ca–P) in lakes and reservoirs in karst areas accounted for more than 40% of the total phosphorus deposited. Thus, submerged plants may contribute to the formation of more Ca–P by mediating calcium carbonate precipitation, thereby increasing the TP content in the sediment (Brenner et al., 2006; O'Connell et al., 2020).

To confirm these conclusions, we investigated the relationship between the aquatic organism structure and Ca–P deposition (Fig. 6). As shown in Fig. 6 A, B, we used the HCO_3^-, CO_2(aq), and Ca^{2+} concentrations of the spring water minus the pond water to represent consumption and added up the monthly consumption for the two study periods to represent the cumulative consumption and found that the cumulative consumption of HCO_3^-, CO_2(aq), and Ca^{2+} was higher in pond water with a higher biomass of submerged plants but lower biomass of algae. Moreover, the calcite saturation index was higher than zero, suggesting that frequent calcium carbonate precipitation occurred in the surface water (Tables S1 and S2; Jiang et al., 2013). Researchers have reported that most submerged plants can use HCO_3^- in water as an inorganic carbon source for photosynthesis, even after $CO_{2(aq)}$ is consumed, thus facilitating the precipitation of calcium carbonate (Dülger et al., 2017; Bao et al., 2022). In addition, the cumulative consumption of Ca^{2+} showed an extremely significant linear positive correlation with Ca–P ($r^2 = 0.78$, $P < 0.01$), which indicated that higher deposition of Ca–P occurred in ponds with high Ca^{2+} concentrations, with more submerged plant biomass producing more Ca–P precipitation by mediating greater precipitation of calcium carbonate (Fig. 6C). This conclusion is supported by the significantly higher Ca–P content in ponds with higher submerged biomass (Table 1, Fig. 4). Zhang et al. (2017) reported that the sediment of Taihu Lake, which is dominated by planktonic algae, was dominated by biogenic P, whereas the sediment of a lake dominated by submerged plants was dominated by calcium-bound P and residual P. Ca–P is redox-insensitive and hardly

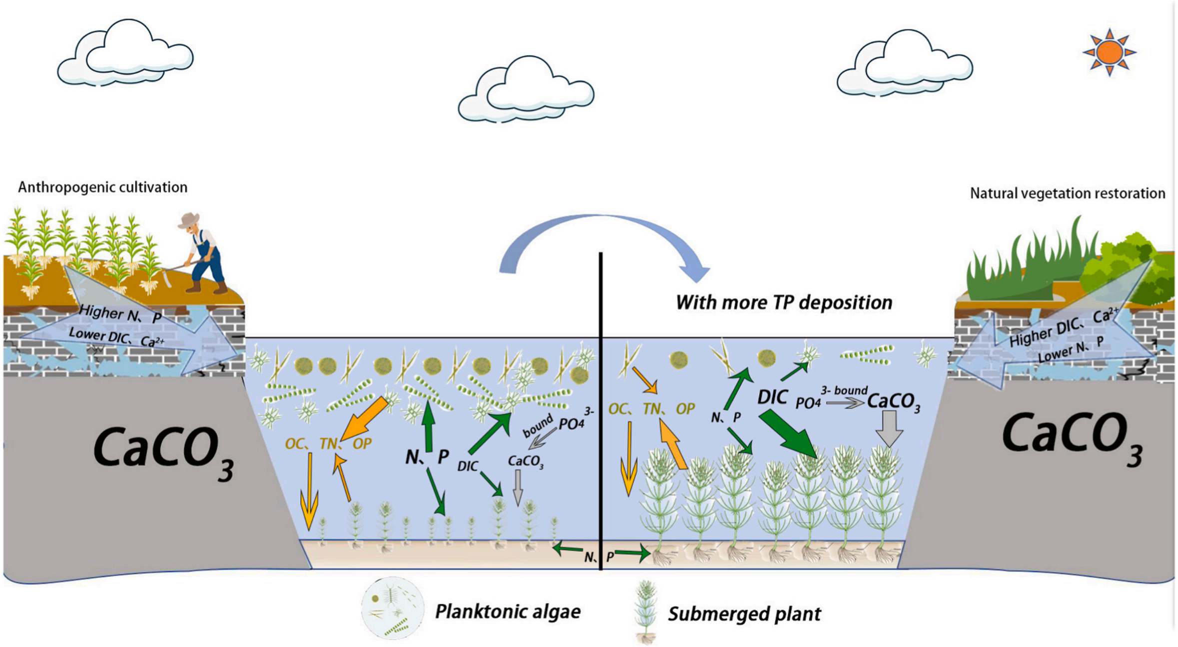

Fig. 7. Conceptual model diagram showing the effects of land use management: the shift of cultivated land to grassland and shrubland by natural vegetation restoration is conducive to the formation of benign aquatic ecosystems and stable organic carbon, nitrogen, and phosphorus sinks in karst surface water due to DIC fertilization.

soluble; thus, it is considered to be a stable form of P (Parsons et al., 2017; Klamt et al., 2019). Wen et al. (2022) found that submerged plant-derived humic acid is more conducive to phosphate retention in sediments than planktonic alga-derived humic acid. Brenner et al. (2006) reported that the productivity of submerged plants and the periphyton communities could also promote P deposition. Additionally, submerged plants promote dissolved oxygen production, which drives the co-precipitation of calcium carbonate with P released from Fe-bound P and biogenic P (Xu et al., 2013; Bai et al., 2020). Therefore, submerged plants can promote more P deposition and stabilization than planktonic algae in some cases (Carey and Rydin, 2011; Kufel et al., 2013; Zhang et al., 2017).

4.3. Effect of land uses on the burial potential of OC, N, and P in karst shallow surface water

Land use change alters the export of DIC, N, and P from watersheds, thereby affecting the biomass and community structure of aquatic photosynthetic organisms in surface waters (Hayes et al., 2015; Luo et al., 2020; Wang et al., 2020a). Previous study showed that ponds associated with grassland and shrubland were characterized by higher DIC and Ca^{2+}, lower N and P, lower planktonic algae biomass, and higher submerged plant biomass, whereas ponds associated with cultivated land and bare soil were characterized by relatively lower DIC and Ca^{2+}, higher N, and P, lower submerged plant biomass, and higher planktonic algae biomass (Bao et al., 2020, 2022). This research found that OC and TN deposition in shrubland and grassland ponds showed small difference from that in cultivated land and bare soil ponds (Fig. 2). However, previous studies have shown that cultivated land increases the export of N and P to water, thus causing eutrophication and increasing the deposition of nitrogen and phosphorus (Downing et al., 2008; Huang et al., 2018; Rogers et al., 2022). We think that this discrepancy is mainly due to the water in these previous studies reaching eutrophic levels and presenting Chl-a concentrations above 20 μg/L, whereas the water in the cultivated land ponds in our study had not yet reached eutrophic levels and presented Chl-a concentrations of only approximately 3 μg/L; thus, lower OC and TN deposition was observed (Huang et al., 2014). Moreover, because the bedrock in the karst area is carbonate rock, the strong soil respiration of shrubland and grassland causes the groundwater to exert a strong dissolution effect on the bedrock, thereby raising the DIC concentration of surface water, which promotes the increase in submerged plant biomass and OC and N deposition; thus, these land uses do not show significant differences in OC and N deposition from that of cultivated land (Table 1, Fig. 2, Dülger et al., 2017; Bao et al., 2022).

In this study, the P content in the deposits to ponds associated with five land uses exhibited different characteristics from the OC and TN content (Fig. 2). TP and Ca–P were generally higher in the deposits under grassland and shrubland. This finding was attributed to the increased export of DIC and Ca^{2+} from the groundwater, which promoted the biomass of submerged plants and precipitation of calcium carbonate in the corresponding surface water, ultimately resulting in increased biogenic P and Ca–P contributed by submerged plants and their periphyton communities (Table 1, Fig. 6, Brenner et al., 2006; Jiang et al., 2013; Zhang et al., 2017; Klamt et al., 2019). It is worth noting that despite the low concentrations of N and P in the surface water of shrublands and grasslands, the biomass of submerged plants remained high, which was mainly because submerged plants can rely on both sediment and water to absorb nutrients (Barko et al., 1991; Barbosa et al., 2020).

Karst landscapes are widely distributed in China; however, their fragile habitats have been severely damaged by human reclamation (Tong et al., 2018; Li et al., 2021). Under governmental initiatives, large-scale projects to return cultivated land to forests and grasslands have been widely carried out (Yue et al., 2020). In this study, it found that OC and TN deposition in ponds associated with shrubland and grassland in karst areas showed small differences from that in ponds associated with cultivated land and bare soil, whereas TP deposition was significantly higher in the ponds associated with shrubland and grassland, which was caused mainly by differences in the physiochemical parameters in the surface water and the community structure of aquatic photosynthetic organisms. Based on the above discussion, this study suggest that natural or artificial restoration of degraded cultivated and bare soil to grassland and shrubland is conducive to the formation of benign aquatic ecosystems and stable OC, N, and P sinks in karst shallow surface waters, and the specific mechanism is shown in Fig. 7.

5. Conclusion

In this study, the characteristics and mechanisms of OC, TN, and TP deposition were investigated in karst shallow surface water under five different land uses. Our results showed that OC and TN deposition showed small differences among ponds associated with the five land uses, whereas TP and Ca–P deposition was significantly higher in the shrubland and grassland ponds than the cultivated land and bare soil ponds. The analysis indicated that the cultivated land, shrubland, and grassland ponds showed small differences in terms of OC and N deposition because the high DIC in the water of the shrubland and grassland ponds promoted submerged plant biomass and OC, TN deposition. Moreover, this study also found that the increased export of DIC and Ca^{2+} from grassland and shrubland groundwater promoted the growth of submerged plants and the precipitation of calcium carbonate in the corresponding surface waters, thereby increasing the biogenic P and Ca–P contributions, which ultimately resulted in higher TP and Ca–P deposition in the traps of ponds associated with shrubland and grassland than with the other three land uses. This suggest that effective land use management (such as the shift of cultivated land and bare soil to grassland and shrubland) is conducive to the formation of benign aquatic ecosystems and stable OC, N, and P sinks in karst surface waters. Additionally, This study may provide further guidance for regulating the burial and stability of OC and nutrients in karst shallow surface waters through land use management at the watershed scale, which has significant implications for eutrophication control and carbon neutralization.

Declaration of competing interest

The authors declare that they have no known competing financial interests or personal relationships that could have appeared to influence the work reported in this paper.

Data availability

Data will be made available on request.

Acknowledgements

This study was financially supported by the National Natural Science Foundation of China (41977298, 42072278, 42130501, 42141008, and 42177248), the Strategic Priority Research Program of Chinese Academy of Sciences (XDB40020000).

Appendix A. Supplementary data

Supplementary data to this article can be found online at https://doi.org/10.1016/j.envres.2023.115488.

References

Asaeda, T., Rajapakse, L., Sanderson, B., 2007. Morphological and reproductive acclimations to growth of two charophyte species in shallow and deep water. Aquat. Bot. 86 (4), 393–401.

Anderson, N.J., Bennion, H., Lotter, A.F., 2014. Lake eutrophication and its implications for organic carbon sequestration in Europe. Global Change Biol. 20 (9), 2741–2751.

Bai, G., Zhang, Y., Yan, P., et al., 2020. Spatial and seasonal variation of water parameters, sediment properties, and submerged macrophytes after ecological restoration in a long-term (6 year) study in Hangzhou west lake in China: submerged macrophyte distribution influenced by environmental variables. Water Res. 186, 116379.

Bao, Q., Liu, Z., Zhao, M., et al., 2020. Primary productivity and seasonal dynamics of planktonic algae species composition in karst surface waters under different land uses. J. Hydrol. 591, 125295.

Bao, Q., Liu, Z., Zhao, M., et al., 2022. Role of carbon and nutrient exports from different land uses in the aquatic carbon sequestration and eutrophication process. Sci. Total Environ. 813, 151917.

Barko, J.W., Gunnison, D., Carpenter, S.R., 1991. Sediment interactions with submersed macrophyte growth and community dynamics. Aquat. Bot. 41 (1–3), 41–65.

Barbosa, V.V., Severiano, J.S., de Oliveira, D.A., et al., 2020. Influence of submerged macrophytes on phosphorus in a eutrophic reservoir in a semiarid region. J. Limnol. 79 (2).

Brenner, M., Hodell, D.A., Leyden, B.W., et al., 2006. Mechanisms for organic matter and phosphorus burial in sediments of a shallow, subtropical, macrophyte-dominated lake. J. Paleolimnol. 35 (1), 129–148.

Brezonik, P.L., Engstrom, D.R., 1998. Modern and historic accumulation rates of phosphorus in Lake Okeechobee, Florida. J. Paleolimnol. 20 (1), 31–46.

Brothers, S.M., Hilt, S., Attermeyer, K., et al., 2013. A regime shift from macrophyte to phytoplankton dominance enhances carbon burial in a shallow, eutrophic lake. Ecosphere 4 (11), 1–17.

Carey, C.C., Rydin, E., 2011. Lake trophic status can be determined by the depth distribution of sediment phosphorus. Limnol. Oceanogr. 56 (6), 2051–2063.

Carpenter, S.R., Cottingham, K.L., Schindler, D.E., 1992. Biotic feedbacks in lake phosphorus cycles. Trends Ecol. Evol. 7 (10), 332–336.

Carvalho, L., McDonald, C., de Hoyos, C., et al., 2013. Sustaining recreational quality of European lakes: minimizing the health risks from algal blooms through phosphorus control. J. Appl. Ecol. 50 (2), 315–323.

Chen, B., Yang, R., Liu, Z., et al., 2017. Coupled control of land uses and aquatic biological processes on the diurnal hydrochemical variations in the five ponds at the Shawan Karst Test Site, China: implications for the carbonate weathering-related carbon sink. Chem. Geol. 456, 58–71.

Chen, J., Yu, J., Bai, X., et al., 2020. Fragility of karst ecosystem and environment: long-term evidence from lake sediments. Agric. Ecosyst. Environ. 294, 106862.

Cruz, J.V., Pacheco, D., Porteiro, J., et al., 2015. Sete Cidades and Furnas lake eutrophication (São Miguel, Azores): analysis of long-term monitoring data and remediation measures. Sci. Total Environ. 520, 168–186.

Downing, J.A., Cole, J.J., Middelburg, J.J., et al., 2008. Sediment organic carbon burial in agriculturally eutrophic impoundments over the last century. Global Biogeochem. Cycles 22 (1).

Dülger, E., Heidbüchel, P., Schumann, T., et al., 2017. Interactive effects of nitrate concentrations and carbon dioxide on the stoichiometry, biomass allocation and growth rate of submerged aquatic plants. Freshw. Biol. 62 (6), 1094–1104.

Enríquez, S., Duarte, C.M., Sand-Jensen, K., 1993. Patterns in decomposition rates among photosynthetic organisms: the importance of detritus C: N: P content. Oecologia 94 (4), 457–471.

Ford, D., Williams, P.D., 2013. Karst Hydrogeology and Geomorphology. John Wiley & Sons.

Hayes, N.M., Vanni, M.J., Horgan, M.J., et al., 2015. Climate and land use interactively affect lake phytoplankton nutrient limitation status. Ecology 96 (2), 392–402.

He, H., Liu, Z., Chen, C., et al., 2020. The sensitivity of the carbon sink by coupled carbonate weathering to climate and land-use changes: sediment records of the biological carbon pump effect in Fuxian Lake, Yunnan, China, during the past century. Sci. Total Environ. 720, 137539.

Hilton, J., O'Hare, M., Bowes, M.J., et al., 2006. How green is my river? A new paradigm of eutrophication in rivers. Sci. Total Environ. 365 (1–3), 66–83.

Howarth, R., Chan, F., Conley, D.J., et al., 2011. Coupled biogeochemical cycles: eutrophication and hypoxia in temperate estuaries and coastal marine ecosystems. Front. Ecol. Environ. 9 (1), 18–26.

Howarth, R.W., Marino, R., 2006. Nitrogen as the limiting nutrient for eutrophication in coastal marine ecosystems: evolving views over three decades. Limnol. Oceanogr. 51 (1part2), 364–376.

Huang, C., Zhang, L., Li, Y., et al., 2018. Carbon and nitrogen burial in a plateau lake during eutrophication and phytoplankton blooms. Sci. Total Environ. 616, 296–304.

Huang, C., Wang, X., Yang, H., et al., 2014. Satellite data regarding the eutrophication response to human activities in the plateau lake Dianchi in China from 1974 to 2009. Sci. Total Environ. 485, 1–11.

Huang, S., Pu, J., Li, J., et al., 2020. Sources, variations, and flux of settling particulate organic matter in a subtropical karst reservoir in Southwest China. J. Hydrol. 586, 124882.

Hu, N., Li, H., Tang, Z., et al., 2016. Community size, activity and C: N stoichiometry of soil microorganisms following reforestation in a Karst region. Eur. J. Soil Biol. 73, 77–83.

Hunter, R.D., 1976. Changes in carbon and nitrogen content during decomposition of three macrophytes in freshwater and marine environments. Hydrobiologia 51 (2), 119–128.

Hupfer, M., Gtichter, R., Ruegger, R.H.R., 1995. Polyphosphate in lake sediments: 31P NMR spectroscopy as a tool for its identification. Limnol. Oceanogr. 40 (3), 610–617.

Jiang, Y., Hu, Y., Schirmer, M., 2013. Biogeochemical controls on daily cycling of hydrochemistry and δ13C of dissolved inorganic carbon in a karst spring-fed pool. J. Hydrol. 478, 157–168.

Jones, J.I., Young, J.O., Eaton, J.W., et al., 2002. The influence of nutrient loading, dissolved inorganic carbon and higher trophic levels on the interaction between submerged plants and periphyton. J. Ecol. 90 (1), 12–24.

Klamt, A.M., Hilt, S., Moros, M., et al., 2019. The effect of a shift from macrophyte to phytoplankton dominance on phosphorus forms and burial in the sediments of a shallow hard-water lake. Biogeochemistry 143 (3), 371–385.

Kufel, L., Biardzka, E., Strzałek, M., 2013. Calcium carbonate incrustation and phosphorus fractions in five charophyte species. Aquat. Bot. 109, 54–57.

Li, S.L., Liu, C.Q., Chen, J.A., et al., 2021. Karst ecosystem and environment: characteristics, evolution processes, and sustainable development. Agric. Ecosyst. Environ. 306, 107173.

Liu, Y., Chen, G., Meyer-Jacob, C., et al., 2021. Land-use and climate controls on aquatic carbon cycling and phototrophs in karst lakes of southwest China. Sci. Total Environ. 751, 141738.

Liu, Z., Macpherson, G.L., Groves, C., et al., 2018. Large and active CO_2 uptake by coupled carbonate weathering. Earth Sci. Rev. 182, 42–49.

Luo, Z., Shao, Q., Zuo, Q., et al., 2020. Impact of land use and urbanization on river water quality and ecology in a dam dominated basin. J. Hydrol. 584, 124655.

Meyers, P.A., 1994. Preservation of elemental and isotopic source identification of sedimentary organic matter. Chem. Geol. 114 (3–4), 289–302.

Murphy, T.P., Hall, K.J., Yesaki, I., 1983. Coprecipitation of phosphate with calcite in a naturally eutrophic lake. Limnol. Oceanogr. 28 (1), 58–69.

Némery, J., Gratiot, N., Doan, P.T.K., et al., 2016. Carbon, nitrogen, phosphorus, and sediment sources and retention in a small eutrophic tropical reservoir. Aquat. Sci. 78 (1), 171–189.

O'Connell, D.W., Ansems, N., Kukkadapu, R.K., et al., 2020. Changes in sedimentary phosphorus burial following artificial eutrophication of Lake 227, Experimental Lakes Area, Ontario, Canada. J. Geophys. Res.: Biogeosciences 125 (8), e2020JG005713.

O'Hare, M.T., Baattrup-Pedersen, A., Baumgarte, I., et al., 2018. Responses of aquatic plants to eutrophication in rivers: a revised conceptual model. Front. Plant Sci. 9, 451.

Parsons, C.T., Rezanezhad, F., O'Connell, D.W., et al., 2017. Sediment phosphorus speciation and mobility under dynamic redox conditions. Biogeosciences 14 (14), 3585–3602.

Rogers, M.N., Williamson, T.J., Knoll, L.B., et al., 2022. Temporal patterns in sediment, carbon, and nutrient burial in ponds associated with changing agricultural tillage. Biogeochemistry 1–16.

Ruban, V., López-Sánchez, J.F., Pardo, P., et al., 2001. Development of a harmonised phosphorus extraction procedure and certification of a sediment reference material. J. Environ. Monit. 3 (1), 121–125.

Schindler, D.W., Carpenter, S.R., Chapra, S.C., et al., 2016. Reducing phosphorus to curb lake eutrophication is a success. Environ. Sci. Technol. 50 (17), 8923–8929.

Seitzinger, S.P., Mayorga, E., Bouwman, A.F., et al., 2010. Global river nutrient export: a scenario analysis of past and future trends. Global Biogeochem. Cycles 24 (4).

Smith, V.H., 2003. Eutrophication of freshwater and coastal marine ecosystems a global problem. Environ. Sci. Pollut. Control Ser. 10 (2), 126–139.

Sun, H., Han, C., Liu, Z., et al., 2022. Nutrient limitations on primary productivity and phosphorus removal by biological carbon pumps in dammed karst rivers: implications for eutrophication control. J. Hydrol., 127480

Thomas, K.A., Hand, L.H., 2011. Assessing the potential for algae and macrophytes to degrade crop protection products in aquatic ecosystems. Environ. Toxicol. Chem. 30 (3), 622–631.

Tong, X., Brandt, M., Yue, Y., et al., 2018. Increased vegetation growth and carbon stock in China karst via ecological engineering. Nat. Sustain. 1 (1), 44–50.

Urbaniak, J., 2010. Estimation of carbonate and element content in charophytes-methods of determination. Pol. J. Environ. Stud. 19 (2).

Wang, H.J., Wang, H.Z., Liang, X.M., et al., 2016. Macrophyte species strongly affects changes in C, N, and P stocks in shallow lakes after a regime shift from macrophyte to phytoplankton dominance. Inland Waters 6 (3), 449–460.

Wang, P., Ma, J., Wang, X., et al., 2020a. Rising atmospheric CO2 levels result in an earlier cyanobacterial bloom-maintenance phase with higher algal biomass. Water Res. 185, 116267.

Wang, S.J., Liu, Q.M., Zhang, D.F., 2004. Karst rocky desertification in southwestern China: geomorphology, land use, impact and rehabilitation. Land Degrad. Dev. 15 (2), 115–121.

Wang, Z., Yin, J.J., Pu, J., et al., 2020b. Integrated understanding of the Critical Zone processes in a subtropical karst watershed (Qingmuguan, Southwestern China): hydrochemical and isotopic constraints. Sci. Total Environ. 749, 141257.

Wen, S.L., Lu, Y.H., Luo, C.Y., et al., 2022. Adsorption of humic acids to lake sediments: compositional fractionation, inhibitory effect of phosphate, and implications for lake eutrophication. J. Hazard Mater. 433, 128791.

Xu, D., Ding, S., Li, B., et al., 2013. Speciation of organic phosphorus in a sediment profile of Lake Taihu I: chemical forms and their transformation. J. Environ. Sci. 25 (4), 637–644.

Yan, Y., Dai, Q., Yuan, Y., et al., 2018. Effects of rainfall intensity on runoff and sediment yields on bare slopes in a karst area, SW China. Geoderma 330, 30–40.

Yuan, H., Tai, Z., Li, Q., et al., 2020. Characterization and source identification of organic phosphorus in sediments of a hypereutrophic lake. Environ. Pollut. 257, 113500.

Yue, Y., Liao, C., Tong, X., et al., 2020. Large-scale reforestation of farmlands on sloping hills in South China karst. Landsc. Ecol. 35 (6), 1445–1458.

Zeng, Q., Liu, Z., Chen, B., et al., 2017. Carbonate weathering-related carbon sink fluxes under different land uses: a case study from the Shawan Simulation Test Site, Puding, Southwest China. Chem. Geol. 474, 58–71.

Zhao, H., Jiang, Y., Xiao, Q., et al., 2021. Coupled carbon-nitrogen cycling controls the transformation of dissolved inorganic carbon into dissolved organic carbon in karst aquatic systems. J. Hydrol. 592, 125764.

Zhao, M., Zeng, C., Liu, Z., et al., 2010. Effect of different land use/land cover on karst hydrogeochemistry: a paired catchment study of Chenqi and Dengzhanhe, Puding, Guizhou, SW China. J. Hydrol. 388 (1–2), 121–130.

Zhang, R., Chen, J., Wang, L., et al., 2017. Characteristics of phosphorus components in surface sediments from a Chinese shallow eutrophic lake (Lake Taihu): new insights from chemical extraction and 31P NMR spectroscopy. Environ. Sci. Pollut. Control Ser. 24 (30), 23518–23527.